Journal of Orthopaedic Research
10:845–853 Raven Press, Ltd., New York

Effects of Material Properties of Femoral Hip Components on Bone Remodeling

Harrie Weinans, Rik Huiskes, and *Henk J. Grootenboer

*Biomechanics Section, Institute of Orthopedics, University of Nijmegen, Nijmegen; and *Department of Biomedical Engineering, Faculty of Mechanical Engineering, University of Twente, Twente, The Netherlands*

Summary: Bone loss around femoral hip stems is one of the problems threatening the long-term fixation of uncemented stems. Many believe that this phenomenon is caused by reduced stresses in the bone (stress shielding). In the present study the mechanical consequences of different femoral stem materials were investigated using adaptive bone remodeling theory in combination with the finite element method. Bone-remodeling in the femur around the implant and interface stresses between bone and implant were investigated for fully bonded femoral stems. Cemented stems (cobalt–chrome or titanium alloy) caused less bone resorption and lower interface stresses than uncemented stems made from the same materials. The range of the bone resorption predicted in the simulation models was from 23% in the proximal medial cortex surrounding the cemented titanium alloy stem to 76% in the proximal medial cortex around the uncemented cobalt–chrome stem. Very little bone resorption was predicted around a flexible, uncemented "iso-elastic" stem, but the proximal interface stresses increased drastically relative to the stiffer uncemented stems composed of cobalt–chrome or titanium alloy. However, the proximal interface stress peak was reduced and shifted during the adaptive remodeling process. The latter was found particularly in the stiffer uncemented cobalt–chrome–molybdenum implant and less for the flexible isoelastic implant. **Key Words:** Total hip replacement—Bone remodeling—Stress shielding—Stress analysis—Bone resorption.

Despite the great success of total hip arthroplasty, long-term fixation is still a major problem. Recently, Ahnfelt et al. (1) showed that different types of total hip arthroplasty systems can have considerably different survival rates. The origin of failure of an orthopedic implant is complex, and many biological and mechanical causative factors interact to induce clinical failure.

The function of total hip arthroplasty is to transfer load from the acetabulum to the femur and to provide an adequate range of motion and sufficient stability. It is assumed that the stress transfer mechanism plays an important role in the performance and survival rate of the implant. As the stresses in prosthesis, bone, and acrylic cement increase, the possibility for failure in the components increases as well. Excessive interface stresses may cause failure of the interface bond, and this may be associated with clinical failure. Another important failure mechanism arises from adaptive bone remodeling in which the bone morphology adapts to the changed mechanical environment. Unnatural stresses or strains can induce morphological changes and bone atrophy, possibly weakening the bone to the point of failure and creating an unfavorable basis for a

Received July 19, 1991; accepted June 5, 1992.
Address correspondence and reprint requests to Dr. H. Weinans at Biomechanics Section, Institute of Orthopedics, University of Nijmegen, P.O. Box 9101, 6500 HB Nijmegen, The Netherlands.

revision arthroplasty. This problem is clinically important, particularly with the use of uncemented implants (16,23,27).

Sarmiento et al. (24) compared titanium alloy (low-modulus) femoral stems with similarly designed high-modulus stems used in cemented total hip arthroplasty. Their data demonstrated a lower incidence of calcar resorption for the low-modulus material. However, later it was found that loosening occurred more frequently with the low-modulus stems. Jakim et al. (15) showed that the use of an extremely low modulus (isoelastic) material is not beneficial in uncemented total hip arthroplasty, because it results in high failure rates due to mechanical loosening. However, bone resorption was rare; mild forms were found in only a few cases. Maloney et al. (17) found marked resorption several years postoperatively in autopsy-retrieved femurs with a cemented stem. They also showed that complete resorption of the bone is unusual, even 17 years after surgery, and that the functional strains will not be restored to the natural level. It is generally believed that these reduced strains (or stresses), usually referred to as stress shielding, are the causes for bone resorption. In animal experiments, even complete resorption of bone surrounding an implant has been reported (18,27).

Adaptive bone-remodeling processes have been studied by a number of investigators (2,4,7,8,12,13, 20,30). They all assumed that this process is regulated by mechanical stimuli detected by sensors within the bone. Integrated with hormonal, genetic, and metabolic factors, this causes bone apposition or resorption, by osteoblasts and osteoclasts. This feedback control process is assumed to converge to a homeostatic equilibrium. Normal loading, and consequently a normal stimulus distribution, leads to a homeostatic equilibrium with normal bone morphology, in which the amount of bone formation is balanced by the amount of bone resorption. An unnatural load alters the stimulus patterns and adaptive bone-remodeling leads to a new equilibrium state. A similar process occurs when a femoral hip component is placed into the femoral canal, because this affects stress and strain patterns in the surrounding bone (12,13,20,31).

By integrating the finite element method with a mathematical description of the bone-remodeling process, it is possible to predict the amount of bone resorption or formation (4,9,13,20,31). In this article, adaptive bone-remodeling simulations in relatively simple two-dimensional finite element models of different femur/stem configurations are used. The first question raised is, will it be possible with a bone-remodeling/finite element method computer model to predict realistic bone remodeling patterns of the femoral bone around a stem? If the answer is yes, it would, in theory, be possible to test prosthetic designs prior to clinical use and to evaluate mechanical effects of certain design features, such as material properties and shape. The aim of this study was to estimate the effects on bone remodeling of different stem materials (high vs. low modulus) for both cemented and uncemented stems.

METHODS

In the present analyses, the apparent density of the bone is used as the only descriptor of the internal bone morphology. It is assumed that the strain–energy per unit of bone mass is the mechanical stimulus that regulates the remodeling process (2,4,9, 30). Hence, both the internal morphology of the bone and the actual mechanical loading condition on the bone are described with scalar quantities (apparent density and strain–energy).

To simulate adaptive bone remodeling in a computer model, a mathematical description of this process is combined with the finite element method. The finite element method provides the stress (σ_{ij}) and strain components (ϵ_{ij}) in each location (per element) of the bone structure. The fundamental assumption of the current bone remodeling theory is that each sensor in the bone strives to bring its strain–energy per unit of bone mass (the remodeling stimulus) to a preset value, the reference stimulus k. In principle, this reference stimulus can be dependent on location, hence site specific (5,13,14,31), although in the present application this reference has a constant value in each location; therefore, the present remodeling theory is regarded as non–site specific (2,9,13,20,30). In a continuum model, the local strain–energy per unit of bone mass can be approximated by U/ρ, where U is the strain–energy density (strain–energy per unit of volume) and ρ is the apparent density (bone mass per unit of volume). When the strain–energy density U is given in MPa and the apparent density ρ in g/cm^3 the stimulus S (U/ρ) is, as a consequence, expressed in J/g. Of course, the strain–energy density U varies in each location over time, due to variations of the hip and muscle loads. In order to take some of these variations into account, the stimulus S is calculated from a number of loading cases (4) by

$$S = \frac{1}{n}\sum_{i=1}^{n}\left(\frac{U_i}{\rho}\right)$$

Hence, for n load cases it takes n finite element method calculations to determine the stimulus. The strain–energy density U is sampled at the centroid of each element, which can be calculated from averaging the strain–energy density values as calculated in the four integration points of an element from $(\sigma_{ij} \cdot \epsilon_{ij})/2$.

Frost (7) suggested that the bone-remodeling process would not react to a small deviation in the mechanical stimulus. He proposed inhibitory values or threshold levels (for the remodeling signal) for both apposition and resorption. Hence, the bone will not respond with apposition or resorption as long as the signal is between these threshold values. This hypothesis was incorporated later in bone-remodeling theories as a "lazy zone" or "dead zone" in the bone response (2,13,31). Mathematically this can be described by an inactive area around the reference stimulus k by introducing a parameter s with $k(1 \pm s)$ representing the dead zone. A relation as shown in Fig. 1, between the rate of density change ($d\rho/dt$) and the stimulus (U_a/ρ) is assumed. Such a relation can be mathematically described by the following expressions:

$$\frac{d\rho}{dt} = A\{S - k(1 + s)\}^2 \quad \text{if} \quad S \geq k(1 + s) \tag{1a}$$

$$\frac{d\rho}{dt} = A\{S - k(1 - s)\}^3 \quad \text{if} \quad S \leq k(1 - s) \tag{1b}$$

$$\frac{d\rho}{dt} = 0 \quad \text{if} \quad k(1 - s) < S < k(1 + s) \tag{1c}$$

$$0\ \text{g/cm}^3 < \rho < 1.74\ \text{g/cm}^3 \tag{1d}$$

where A is a time constant and k is the (constant) reference stimulus. The exponent for bone apposition is taken as 2 (Eq. 1a), whereas the exponent for resorption is taken as 3 (Eq. 1b). This reflects the finding that resorption occurs more progressively than apposition (21). Equation 1d reflects the fact that bone can only vary its density between zero density and the density of cortical bone.

Equation 1 can be solved by means of forward Euler integration with constant time-steps (Δt) in the finite element method computer procedure, and the density change per time step is calculated from

$$\Delta\rho = A\,\Delta t\{S - k(1 \pm s)\}^{\alpha} \quad \text{if} \quad S \geq k(1 + s) \quad \text{or} \quad S \leq k(1 - s) \tag{2}$$

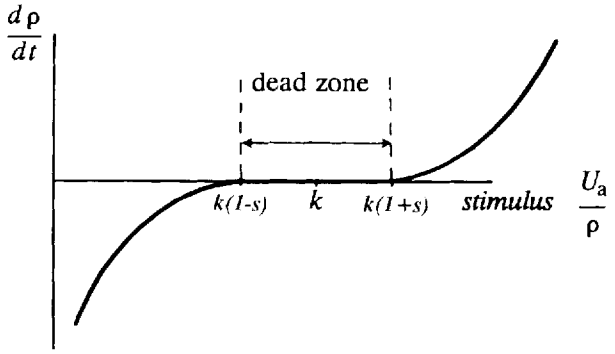

FIG. 1. Nonlinear remodeling relation between the amount of bone apposition or resorption ($d\rho/dt$) and the remodeling stimulus (S).

where α takes the value 2 or 3. The product $A\Delta t$ was taken as 30.0, which is small enough to ensure convergence of the solution procedure (30).

The density of the bone is related to the elastic modulus (E) according to

$$E = 3{,}790\rho^3 \tag{3}$$

whereby the elastic modulus is expressed in MPa and the apparent density in g/cm^3. This relationship is based on the study of Carter and Hayes (3), whereby the strain rate dependency was found to be insignificant for the present application and is arbitrarily chosen as 1.0/s. The elastic modulus and the corresponding density are determined per element in the finite element procedure, with a maximal value of 20,000 MPa (ρ = 1.74 g/cm^3) and a minimal value of 0.008 MPa (ρ = 0.01 g/cm^3). This represents an upper value for the cortical bone density or complete resorption of the bone.

First, this procedure is used to determine the density distribution in a normal proximal femur. A two-dimensional finite element model is constructed with 349 elements in the front plate and 183 elements in the side plate (Fig. 2A), whereby the side plate accounts for the structural contribution of the out-of-plane cortical bone (28). Only the front plate takes part in the remodeling process. The side plate keeps a constant elastic modulus during the simulation (E = 17,000 MPa). We assumed that normal bone has a density distribution such that $d\rho/dt$ in Eq. 1 is zero and the reference stimulus k = 0.0025 J/g. The value of k is chosen by tuning, in accordance with previous studies with the same model (12,30), where it was found that it produces a realistic bone morphology. There is no dead zone assumed for the generation of normal bone morphol-

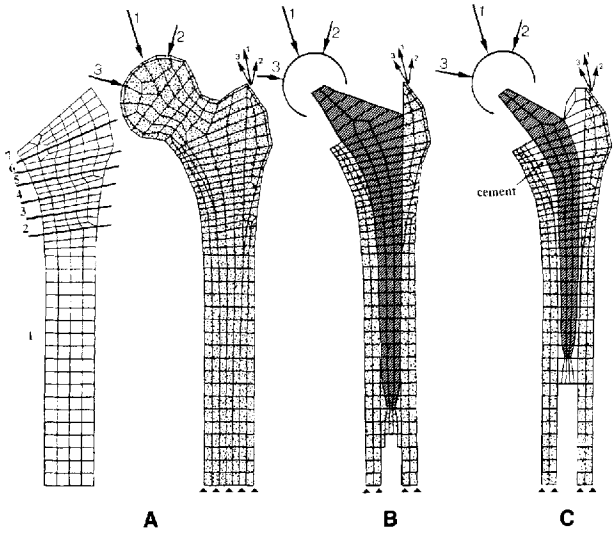

FIG. 2. The finite element method meshes as used in the different simulation analyses. **A:** Normal femur with side plate. **B:** Uncemented stem. **C:** Cemented stem. The meshes consist of four node linearly elastic and isotropic elements with a linear displacement field along the edges. The magnitudes of the hip joint and hip abductor forces, respectively, are for the different load cases: 1, 2317 N and 702 N; 2, 1548 N and 468 N; 3, 1158 N and 351 N. The directions for the hip joint and abductor force, respectively: 1, 24° and 28° from vertical; 2, 56° and 35° from vertical; 3, 15° and 8° from vertical. The front plate has a thickness of 12 mm for the normal femur model and both the models with stem. The side plate has a nonuniform thickness distribution, decreasing from distal to proximal. In the seven indicated areas, the thicknesses are as follows: area 1, 4.0 mm; area 2, 3.0 mm; area 3, 2.0 mm; area 4, 1.0 mm; area 5, 0.7 mm; area 6, 0.4 mm; area 7, 0.2 mm. All front plate meshes were attached to the same side plate at the entire medial and lateral aspects.

ogy, so s in Eq. 1 is taken as zero. This reflects the assumption that in osteogenesis the objective is satisfied as well as possible. The process is started from a uniform density distribution of 0.8 g/cm^3 for the entire front plate. Three loading cases representing daily activity are chosen (Fig. 2A). The first load case represents the stance phase during gait. The other two loads represent extreme ranges of motion with reduced hip joint reaction and hip abductor forces (4). All loads were applied as distributed loads over four elements.

The solution found from this simulation relative to the normal femur is taken as the initial density distribution and serves as the direct postoperative density distribution in the second model, in which the presence of cemented or uncemented femoral hip components are simulated (Fig. 2B and C). The latter two models were constructed by modifying the original femur model of Fig. 2A. The loads on these two models are identical in direction and magnitude to those in the model of the normal femur. Again, the same side plate is used to account for the out-of-plane cortical bone. The implants were assumed to be completely bonded to the bone or cement; hence, no special interface facilities were applied in the finite element models. Because the prostheses provoke entirely different stress distributions, the bone structure starts remodeling according to Eq. 1. It is assumed that the bone strives for the same reference stimulus k = 0.0025 J/g, within the limits of a dead zone of ±35% of the reference stimulus k (s = 0.35).

For the cemented implant (Fig. 2B), stems made out of cobalt–chrome–molybdenum alloy (CoCrMo) and a titanium alloy are simulated. The thickness of the bone cement is 2.5–6 mm (Fig. 2C) and its elastic modulus was taken as 3,000 MPa. For the uncemented system (Fig. 2B), three different materials were studied: CoCrMo (elastic modulus 210,000 MPa), titanium (110,000 MPa), and a hypothetical material with an elastic modulus in the range of cortical bone (20,000 MPa), a so-called isoelastic material. For all models the effects on bone remodeling were plotted and calculated in percentages in four different areas according to Gruen's zones. The percentage bone loss in a specific volume was calculated as (actual bone mass − initial bone mass)/initial bone mass. In addition, the load transfer between stem and bone was studied by evaluating the interface stresses in the initial configuration and after the remodeling process.

RESULTS

Bone Remodeling

In the bone remodeling prediction of the normal femur model, the reference stimulus value k was tuned such that the best possible fit with a realistic density distribution was found. A larger reference value k produces less bone in the structure and vice versa. Hence, by tuning the value of k, the overall amount of bone in the end configuration can be triggered. The density distribution as predicted in the computer simulation of the proximal femur without prosthesis fits well with normal bone morphology for a reference stimulus value k = 0.0025 J/g, as shown in Fig. 3. For this result the most important aspects of proximal femoral morphology are represented: medial and lateral cortices, intramedullary canal, Ward's triangle, metaphyseal cortical shells, and the characteristic cancellous distributions in the femur head and trochanter.

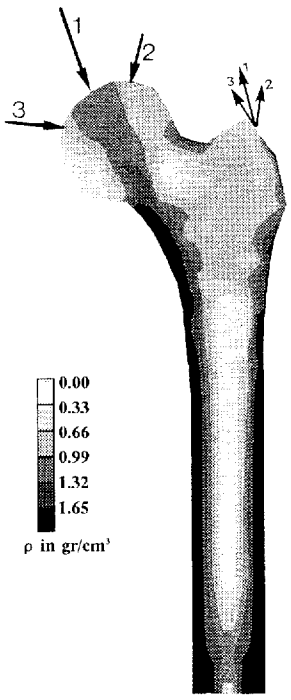

FIG. 3. Density distribution as predicted by the remodeling simulation of the normal femur.

The only other parameter that is tuned for the remodeling predictions of the models with prostheses is the dead zone width s. The smaller the dead zone, the more resorption was predicted. A dead zone of ±35% of the reference stimulus (s = 0.35) was taken, based on a detailed comparison between a simulation of bone-remodeling patterns around uncemented femoral stems in dogs and its experimental counterpart (14). It was found that for s = 0.35, the results of the remodeling patterns with respect to the present study also fit well within a realistic range.

In order to compare the results of bone remodeling around the different stems with the nonremodeled case, the distribution as shown in Fig. 3 is also shown for the modified mesh with prosthesis (Fig. 4A). This can be regarded as the direct postoperative configuration.

The two simulation models with cemented CoCrMo and titanium stems generated mild resorption, predominantly localized in the calcar region (proximal/medial). The differences between resorption patterns around a CoCrMo stem (Fig. 4B) and a titanium stem (Fig. 4C) were not extensive. The percentage bone loss, or apposition (also indicated in Fig. 4), gave 38% as a maximum for the cemented CoCrMo stem, found in the proximal/medial region, versus 23% for the titanium stem in the same area. On the lateral side, the resorption was lower in both cases (18 and 19%) and in the mid-stem region some resorption was predicted only around the CoCrMo stem (5% medial and 11% lateral). The bone resorption predicted around the uncemented CoCrMo or titanium stems was much more severe (Fig. 4D and E). In particular, the CoCrMo stem provoked severe bone loss; up to 76% in the calcar area, 45% in the proximal/lateral region, and ~30% in the medial and lateral mid-stem regions. The resorption predicted around the uncemented titanium stem was still much more severe than around the cemented stems (54% proximal/medial, 38% proximal/lateral, and 4 and 14% in the mid-stem regions). It is clear that stiffer components lead to more extensive

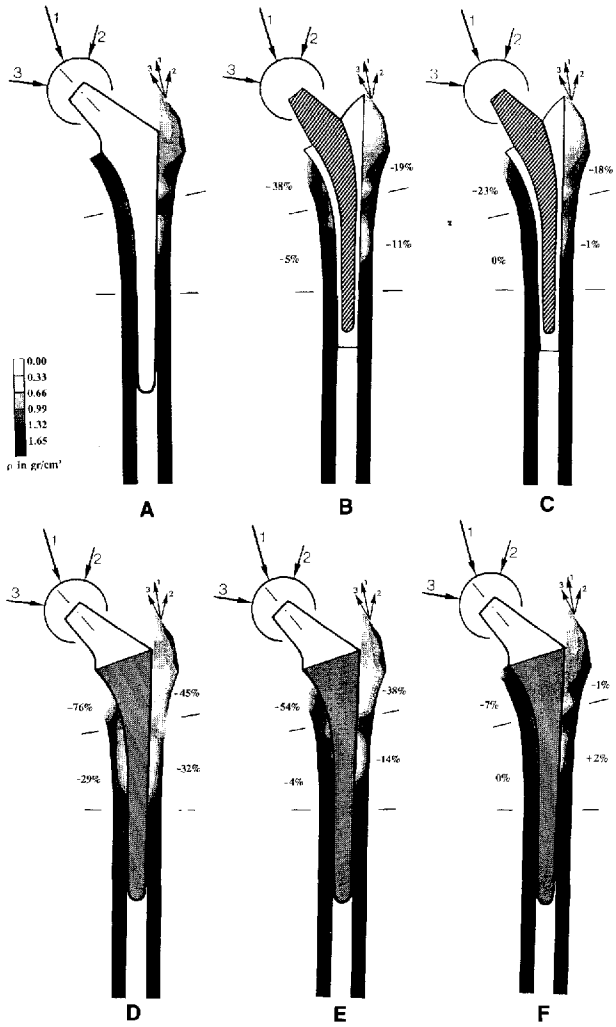

FIG. 4. Density distributions of the proximal femur with different stem types. **A:** Initial postoperative configuration. **B:** Cemented CoCrMo stem. **C:** Cemented titanium stem. **D:** Uncemented CoCrMo stem. **E:** Uncemented titanium stem. **F:** Uncemented isoelastic stem. The percentage bone loss in different areas is indicated, corresponding to the Gruen's zones.

proximal bone resorption. The hypothetical isoelastic prosthesis provoked a small amount of bone loss, restricted to the medial rim of the calcar, directly under the resection level, where 7% resorption was predicted. In the lateral mid-stem region, an increase of bone density of 2% was even predicted.

Load Transfer

The interface stresses between implant and bone were first studied in the initial postoperative configuration. It was found that the load transfer from prosthesis to bone occurs more proximally when the implant is more flexible. This is illustrated in Fig. 5A and B, where the distribution of the strain–energy density in prosthesis and bone is shown for two initial configurations: the most flexible stem (uncemented isoelastic) and the most rigid stem (uncemented CoCrMo). The rigid stem case demonstrates the stress shielding (or strain–energy density shielding) mechanism in the upper bone regions. The strain–energy density values in the proximal regions are relatively low, both in stem and bone, indicating that there is little stress transfer from stem to bone here. The flexible configuration shows much higher strain–energy density values in the upper regions, illustrating that the stem is transferring load directly to the calcar.

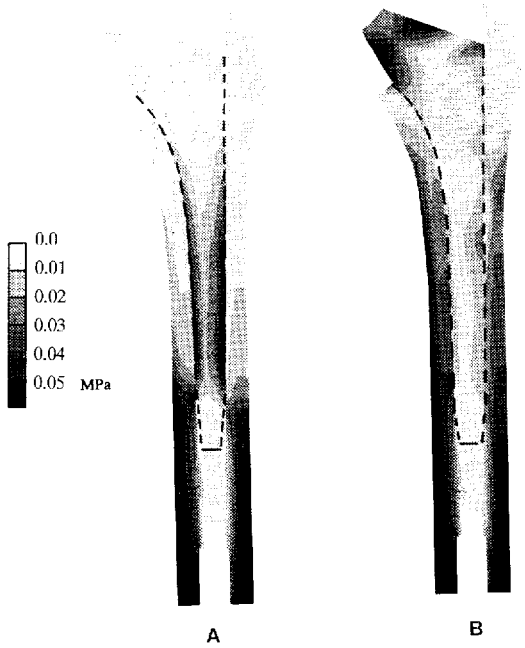

FIG. 5. Strain–energy density distribution in stem and bone with the CoCrMo prosthesis (stiff) **(A)** and the isoelastic prosthesis (flexible) **(B)**. The average strain–energy density from the three different load cases is shown.

The interface stress patterns (normal and shear) showed a proximal and a distal peak in all cases, which is a general pattern for the interface stresses around intramedullary stems (10,11). The two cemented configurations had lower peak stresses than the uncemented configurations, whereby a cemented CoCrMo stem produced slightly lower proximal peak stress than a cemented titanium stem. Comparing the uncemented stems, it appeared that the CoCrMo and the titanium stems generate high interface stresses distally, whereas the isoelastic stem generates high stress proximally. This reflects again the mechanism that more flexible stems transfer the load more proximally, as demonstrated in Fig. 5 and shown in several other studies (10,11,13). Interface shear and normal stresses showed qualitatively similar patterns.

During the remodeling process, however, these interface stress patterns can change significantly. The peak stresses can reduce and shift after the remodeling process. For the stiff uncemented CoCrMo configuration with loading case 1, it was found that the proximal medial interface peak stress decreased from 6.2 to 3.0 MPa and also shifted to distal because of the extensive loss of proximal bone (Fig. 6A). In particular, the models with a severe loss of bone display this extensive interface stress change and shift of peak stress location.

Such a shift in peak stress location was not found in the isoelastic configuration. The interface peak stress was again located at the medial–proximal bone rim, where bone still remained, conversely to the CoCrMo case (compare Fig. 4D and F). However, with this flexible stem a reduction of the proximal peak stress was also found, as demonstrated in Fig. 6B, which shows the interface peak stresses before and after remodeling in the isoelastic configuration. For this configuration an interface peak of 27 MPa was the highest found for load case 1. After remodeling there was a 30% reduction to 18 MPa normal compression at the same location.

DISCUSSION

The results show that it is possible to construct a model that produces realistic bone morphology patterns for both a normal femur and a femur with a prosthesis. All results of the remodeling patterns around the stems fit into a realistic range when compared with clinical data (16,26). When comparing

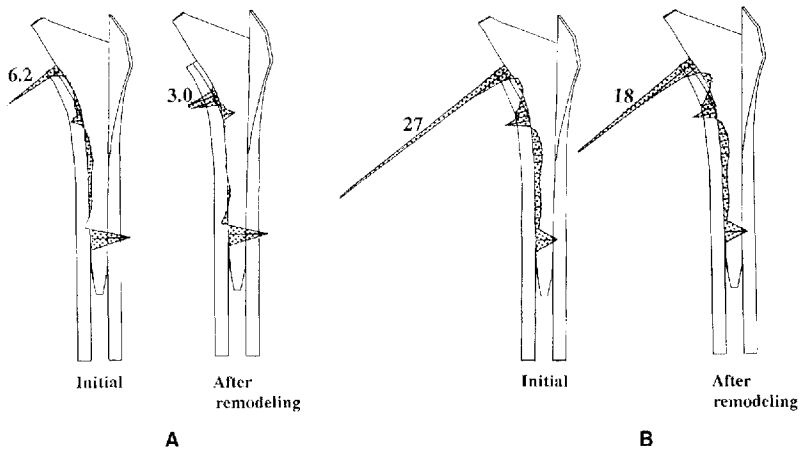

FIG. 6. Normal interface stresses, obtained from the first load case (Fig. 2), before (initial) and after bone remodeling for the CoCrMo **(A)** and isoelastic uncemented stems **(B)**.

the results in relation to each other, the computer simulations confirm the clinical observation that with relatively stiff canal filling stems, severe proximal bone resorption occurs (6). On the other hand, the flexible iso-elastic stem created high proximal interface stresses, increasing the chances for interface debonding and subsequent loosening.

It must be emphasized that the present model is relatively simple when compared with the in vivo situation. Trabecular bone is assumed isotropic and continuous. In reality, the processes we simulate take place at a microstructural level. The finite element model is two dimensional; consequently, only loads acting in the mid-frontal plane can be considered. Nevertheless, the side plate does account for the three-dimensional structural integrity of the cortex, such that a good representation of the behavior in the mid-frontal plane can be obtained (28). The side plate and its specific thickness distribution (Fig. 2) was found to be influential in the generation of the diaphyseal and metaphyseal density distribution. If one is interested only in the distribution of the density patterns in the utmost proximal part of the bone, the function of a side plate is less important, as shown in two-dimensional models of Carter et al. (4) and Beaupré et al. (2), where no link to intramedullary fixation was made. Orr et al. (20) showed that such a model, without a side plate, can contribute to the understanding of the bone-remodeling processes under the cup of a resurfacing femoral component.

Because the front plate is considered in the remodeling analyses only, the plots of Figs. 3–6 refer to the mid-frontal part of the bone. Of course the three applied loads are a simplification of the complex real three dimensional loading patterns. Another important simplification in the analyses is that a perfect fit and completely bonded connections between implant and bone were assumed. This means that all stress components (compression, tension, and shear) can be transferred by the interface. For most cemented implants (when the surface is not polished) this is realistic, certainly directly postoperatively. However, for the uncemented implants perfect fit is not obtained and ingrowth percentages of only 10–20 percent were reported (19,25). Therefore, the present results must be regarded as general trends in an idealized situation. Huiskes (10) showed that the load transfer in relation to completely bonded and partly bonded total hip arthroplasty configurations is not so different, whereas the differences between partly bonded and complete debonding are much more extensive. It must be well understood that our objective was to study the exclusive effects of one parameter, namely the stem material stiffness. Hence, all other parameters, including interface condition, were kept equal in the femur/prosthesis models. Interface stresses should be interpreted with caution. They depend very heavily on local details that are not accounted for in the finite element model. Their interpretation should be based on a comparative evaluation. With respect to mesh refinement, we have found that a more refined mesh would lead to qualitatively similar results (29). All present models converged rapidly to a steady state end configuration (29).

The mathematical description of the bone-remodeling process consists of a set of equations (Eq. 1 and 3) with various parameters. The remodeling relation must be considered as an empirical relationship for which the constants are unknown. The choice of the stimulus (strain–energy per unit of bone mass) is based on the fact that strain–energy is a physical parameter related to the local loading

conditions inside the bone, and is a scalar quantity conversely to stress or strain, hence simple to use. The constant A is related to the size of the time step, which should be small enough so that it will not affect the result. The effect of the exponents 2 and 3 in Eq. 1 is also marginal. We have tried other exponent values, which gave similar results (10). The same can be said of the constants in the modulus density relationship (Eq. 3). It is mentioned several times in the literature that an exponent of 2.0 for cancellous bone would be more accurate (22). It was found that the constants (3,790 and 3.0) in this relationship had an insignificant effect on the result as long as the exponent was larger than 1.0 (29). The only two parameters in the present description that have a significant effect on the results are the reference stimulus k and the dead zone s, which were both tuned in the present model. We first tried a dead zone of zero, which gave good morphological predictions of the normal femur, but the remodeling patterns around the stems gave a severe resorption to such an extent that the complete proximal bone disappeared around a CoCrMo stem (10). The value of 35% for the dead zone s also gave reasonable results in a simulation study of bone remodeling patterns around femoral stems in the canine (14). Of course, these models were different from the present ones and it is uncertain whether a dead zone would be similar in extent for the canine and the human.

The value of the reference stimulus k was determined in the same way, by parametric analysis (12,30). It was also found that the remodeling effects are not very susceptible to the precise loading history used, as long as a reasonable range of both hip and trochanteric loading cases are included and the loads in the total hip arthroplasty models are equal to those in the intact model. The choice of the initial density distribution (uniform with $\rho = 0.8$ g/cm^3) for the generation of the normal bone morphology has only a minor influence on the end configuration (2,30).

It is certainly not easy to match the quantitative values of the present results with clinical radiographic analyses, because conventional radiographic techniques are not precise, and quantitative techniques are not yet widely used. Steinberg et al. (26) showed, using dual-energy radiographic densitometry, that bone loss associated with cemented femoral components may be 40–50% in the area of the lesser trochanter and slightly below. This area corresponds roughly to the proximal medial zone as indicated in Fig. 4, for which 38 and 23% bone loss was found in the computer simulations with the cemented CoCrMo and titanium stems, respectively. Kiratli et al. (16) used a similar technique and reported 20–30% bone loss in some proximal bone regions, up to 5 years after an uncemented femoral stem was placed. The ranges of bone mass reductions found in the present study are similar. Both Kiratli et al. (16) and Steinberg et al. (26) reported ensuing bone loss after more than 3 years of follow-up, which is contradictory to the idea that bone remodeling stabilizes in 2–3 years. Our computer predictions concern stabilized end configurations, whereas in most clinical studies it is uncertain to which extent the observed remodeling patterns can be regarded as having reached equilibrium. Nevertheless, our predictions are similar to these quantitative clinical findings.

The results of the remodeling simulations demonstrate drastic bone resorption around rigid uncemented stems, which would plead for the use of flexible materials. However, if we study the interface stresses, it is found that this is not necessarily a favorable alternative. The proximal medial interface stresses become extremely large in the isoelastic case, which indicates a considerable risk for interface disruption. During the bone-remodeling process this interface stress peak decreases; however, it is still considerably higher than for the stiffer CoCrMo and titanium stems. It may be possible that the interface stresses become so elevated that no permanent ingrowth will occur because of immediate disruption after the slightest ingrowth. In other words, the results show that a flexible, uncemented isoelastic stem would become a favorable option only when the shape of the stem can be designed to guarantee minimal proximal interface stresses, or when interface bonds can be made adequately strong.

Considering the question of titanium versus CoCrMo in light of the present results, it is evident that a design conflict occurs. Titanium generates less bone resorption, but higher proximal interface stresses (10); therefore, greater probability for interface disruption and subsequent relative motion. We do not know precisely how much interface stress the interface can sustain in long-term dynamic loading. However, in view of the amounts of bone resorption predicted in the various cases and the values of the interface stress peaks found, and considering that (coated and ingrown or osseointegrated) stem/bone interfaces tend to be much

stronger than stem/cement and cement/bone interfaces, the relatively stiff CoCrMo stem in the cemented configuration appears to be the best choice. However, titanium would be preferred in uncemented cases where the overall stiffness of a CoCrMo implant would cause gross adverse remodeling.

Acknowledgment: This study was sponsored in part by The Netherlands organization for research (NWO/Medigon) and by Osteonics Corp, New Jersey, U.S.A.

REFERENCES

1. Ahnfelt L, Herberts P, Malchau H, Anderson GBJ: Prognosis of total hip replacement. *Acta Orthop Scand* [*Suppl*] 238, 1990
2. Beaupré GS, Orr TE, Carter DR: An approach for time-dependent bone modeling and remodeling—application: a preliminary remodeling simulation. *J Orthop Res* 8:662–670, 1990
3. Carter DR, Hayes WC: The behavior of bone as a two-phase porous structure. *J Bone Joint Surg* 59A:954–962, 1977
4. Carter DR, Orr TE, Fyhrie DP: Relationships between loading history and femoral cancellous bone architecture. *J Biomech* 22:231–244, 1989
5. Cowin SC, Hegedus DH: Bone remodeling I: theory of adaptive elasticity. *J Elasticity* 6:313–326, 1976
6. Engh CA, Bobyn JD: The influence of stem size and extent of porous coating on femoral bone resorption after primary cementless hip arthroplasty. *Clin Orthop* 231:7, 1988
7. Frost HM: *The Laws of Bone Structure*. Springfield, Charles C. Thomas, 1964
8. Frost HM: Vital biomechanics. Proposed general concepts for skeletal adaptations to mechanical usage. *Calcif Tissue Int* 42:145–156, 1987
9. Fyhrie DP, Carter DR: A unifying principle relating stress to trabecular bone morphology. *J Orthop Res* 4:304–317, 1986
10. Huiskes R: The differing stress patterns of press-fit, ingrown and cemented femoral stems. *Clin Orthop* 261:27–38, 1990
11. Huiskes R: Some fundamental aspects of human-joint replacement. *Acta Orthop Scand* [*Suppl*] 185, 1980
12. Huiskes R, Weinans H, Dalstra M: Adaptive bone remodeling and biomechanical design considerations for noncemented total hip arthroplasty. *Orthopedics* 12:1255, 1989
13. Huiskes R, Weinans H, Grootenboer HJ, Dalstra M, Fudala B, Slooff TJ: Adaptive bone-remodeling theory applied to prosthetic-design analysis. *J Biomech* 20:1135–1150, 1987
14. Huiskes R, Weinans H, Rietbergen B van, Sumner DR, Turner TM, Galante JO: Validation of strain-adaptive bone remodeling analysis to predict bone morphology around noncemented THA. *Trans ORS* 16:105, 1991
15. Jakim I, Barlin C, Sweet MBE: RM isoelastic total hip arthroplasty. *J Arthroplasty* 3:191–199, 1988
16. Kiratli BJ, Heiner JP, McKinley N, Wilson MA, McBeath AA: Bone mineral density of the proximal femur after uncemented total hip arthroplasty. *Trans ORS* 16:545, 1991
17. Maloney WJ, Jasty M, Burke DW, et al.: Biomechanical and histological investigation of cemented total hip arthroplasties. *Clin Orthop Rel Res* 249:129–140, 1989
18. Miller JE, Kelebay LC: Bone ingrowth disuse osteoporosis. *Orthop Trans* 5:380, 1981
19. Noble PC, Alexander JW, Granberry ML, et al.: The myth of 'press-fit' in the proximal femur. Scientific exhibit, 55th AAOS, Atlanta GA, February 4–9, 1988
20. Orr TE, Beaupré GS, Carter DR, Churman DJ: Computer predictions of bone remodeling around porous-coated implants. *J Arthroplasty* 5:191–200, 1990
21. Parfitt AM: The physiologic and clinical significance of bone histomorphometric data. In: *Bone Histomorphometry: Techniques and Interpretation*, ed. by R Recker, Boca Raton, Fl, CRC Press, 1983, pp 143–223
22. Rice JC, Cowin SC, Bowman JA: On the dependence of the elasticity and strength of cancellous bone on apparent density. *J Biomech* 21:155–168, 1988
23. Rosenberg A: Cementless total hip arthroplasty: femoral remodeling and clinical experience. *Orthopaedics* 12:1223–1233, 1989
24. Sarmiento A, Gruen TA: Radiographic analysis of low-modulus titanium-alloy femoral total hip component. *J Bone Joint Surg* 67A:48–56, 1985
25. Schimmel JW, Huiskes R: The primary fit of the Lord cementless total hip. *Acta Orthop Scand* 59:638–642, 1988
26. Steinberg GG, Kearns McCarthy C, Baran DT: Quantification of bone loss of the femur after total hip arthroplasty. *Trans ORS* 16:221, 1991
27. Turner TM, Sumner DR, Urban RM, Rivero MD, Galante JO: A comparative study of porous coatings in a weight-bearing total hip-arthroplasty model. *J Bone Joint Surg* 68A: 1396–1409, 1986
28. Verdonschot N, Huiskes R: FEM analyses of hip prostheses: validity of the 2-D side-plate model and the effects of torsion. *Proceedings of the 7th Meeting of the European Society of Biomechanics*, University of Aarhus, Aarhus, Denmark, 1990, p A20
29. Weinans H, Huiskes R, Grootenboer HJ: The behavior of adaptive bone-remodeling simulation models. *J Biomech* 1992 (in press)
30. Weinans H, Huiskes R, Grootenboer HJ: Convergence and uniqueness of adaptive bone remodeling. *Trans ORS* 14:310, 1989
31. Weinans H, Huiskes R, Grootenboer HJ: A hypothesis concerning minimal bone density threshold levels as final stages of bone remodeling. *Trans ORS* 15:78, 1990